

An Avirulent *Ralstonia Solanacearum* Strain Undergoes Phenotype Conversion from a Pathogenic Strain Under Natural Environment

Deju Chen^{*}, Haifeng Zhang, Yanli Li, Yanpin Chen, Xuefang Zheng, Jieping Wang, Jiamei Che, Bo Liu^{*}

Institute of Agricultural Bioresources, Fujian Academy of Agricultural Sciences, Fuzhou, China

Email address:

chendegu@163.com (Deju Chen), 13600828002@126.com (Haifeng Zhang), 158759666@qq.com (Yanli Li),

cyp071@yahoo.com.cn (Yanpin Chen), zhengxuefang2002@yahoo.com.cn (Xuefang Zheng), wangjieping2011@163.com (Jieping Wang),

chejm2002@163.com (Jiamei Che), fzliubo@163.com (Bo Liu)

^{*}Corresponding author

To cite this article:

Deju Chen, Haifeng Zhang, Yanli Li, Yanpin Chen, Xuefang Zheng, Jieping Wang, Jiamei Che, Bo Liu. An Avirulent *Ralstonia Solanacearum* Strain Undergoes Phenotype Conversion from a Pathogenic Strain Under Natural Environment. *American Journal of Bioscience and Bioengineering*. Vol. 8, No. 3, 2020, pp. 46-58. doi: 10.11648/j.bio.20200803.13

Received: August 8, 2019; Accepted: September 5, 2019; Published: July 4, 2020

Abstract: An avirulent *R. solanacearum* strain named FJAT-1458 was isolated from living tomato vessel and it showed no toxicity to tomato, pepper and eggplant. Multilocus sequence analysis (MLSA) based on eight genes (*egl*, *hrpB*, *mutS*, *pehA*, *recA*, *rpoA*, *rpoB* and *rpoC*) and whole genome average nucleotide identity (ANI) analysis suggested that strain FJAT-1458 belong to phylotype I. Genome sequence of the strain FJAT-1458 revealed a circular chromosome and a circular megaplasmid with whole genome size of 6,059,899 bp and GC content of 66.78%. Functional annotation of FJAT-1458 showed a total of 5,442 genes, with 5,166 protein-encoding genes, 202 pseudogenes and 74 noncoding RNA genes. Among which, 3,938 protein-coding genes can be assigned to 23 COG families, and 1,521 of them had KEGG orthologs. Prophage prediction using PHASTER revealed 12 prophages, including 7 intact, 1 questionable and 4 incomplete prophages. Comparative genome analyses between GMI1000 and FJAT-1458 showed that most of the virulence factors were well conserved and only small portion of them were distinct between them. Two genes, including a methyltransferase and an ISL3 family transposase genes, were identified to be inserted immediately upstream (141 bp) of *phcA* gene, which assumed to be responsible for avirulence of strain FJAT-1458. It is suggested that strain FJAT-1458 was originated from a wild-type pathogenic strain through an accident phenotype conversion, which is like those when cultured under experimental conditions. Our study provides new insight into the evolution of virulence in *R. solanacearum* strain under natural environment.

Keywords: *Ralstonia Solanacearum*, Comparative Genomic Analysis, Virulence Factors, Single Molecular Real-time Sequencing, Phenotype Conversion

1. Introduction

Ralstonia solanacearum is one of the most important bacterial plant pathogens, which causes lethal wilts on more than 200 plant species belonging to over 50 different botanical families over a broad geographical range [1]. The bacterium enters plant roots, invades the xylem vessels and spreads rapidly to aerial parts of the plant through the vascular system where it reproduces in large number within a few days, leading to the death of plant [2]. In addition to its lethality, *R.*

solanacearum is able to survive in soils, waters and under various abiotic stresses for a long period without losing the ability to wilt host plants [3], which makes it even harder to be controlled [4]. Several strategies were employed to control of diseases caused by *R. solanacearum*, including use healthy plant seeds [5], crop rotation for 2-5 years [6], chemical control [1, 7]. An alternative strategy was to use biological control agent such as antagonistic bacteria or avirulent mutants of *R. solanacearum*. However, the promising results could only be obtained under controlled conditions while was

not confirmed in field [7].

R. solanacearum have evolved an elegant and effective system to invade host and expand its plant host range. There are two major pathogenicity determinants exist in *R. solanacearum*, the type III secretion system (T3SS) and extracellular polysaccharide (EPS). T3SS injects the “effector proteins” into the plant cell cytosol to favour infection [8, 9], and EPS is largely responsible for the vascular dysfunction that causes wilt symptoms in susceptible hosts and promotes rapid systemic colonization as well [10]. Besides, *R. solanacearum* produces plenty of other factors that are potentially involved in the infection, including type II secreted plant cell wall-degrading enzymes, motility or attachment appendages, aerotaxis transducers, cellulases and pectinases [11]. The pathogenesis process was controlled through a sophisticated regulatory circuit and the LysR family transcriptional regulator PhcA plays a central role which regulates directly and indirectly many of those virulence genes [12].

Interestingly, under certain growth conditions, some members of the *R. solanacearum* population spontaneously undergo phenotype conversion (PC) from a wild-type pathogenic to a nonpathogenic form when it was allowed to grown to a high concentration [13]. Several genetic studies have revealed that PC is often resulted from mutation in *phcA* gene [14–17]. However, the phenomenon of PC under natural environment has never been reported probably due to that only few avirulent wild-type *R. solanacearum* strains have been identified. In our previous study, a *R. solanacearum* strain named FJAT-1458 has been isolated from living tomato vessel [18].

The objective of this study was to determine if the FJAT-1458 is born with nonpathogenic or the result of PC from a wild-type pathogenic strain. The complete genome sequence of strain FJAT-1458 was determined with single molecular real-time sequencing (SMRT) biotechnology. The genome comparison between strain FJAT-1458 and other *R. solanacearum* strains was performed. Besides, to elucidate the reason why strain FJAT-1458 is avirulent against *Solanaceae* plants, the virulence factors of strain FJAT-1458 were compared with strain GMI1000.

2. Materials and Methods

2.1. Bacterial Strains and Growth Conditions

R. solanacearum strain FJAT-1458 was isolated from living *Solanum lycopersicum* L. vessel from Fuzhou, Fujian, China. The strain was kept frozen in 20% glycerol at -80°C. A single colony was selected from plating of a culture of FJAT-1458 on tetrazolium chloride agar medium (TZC) [19] and the pure colony was then grown at 30±2°C in liquid SPA medium (sucrose, 20 g; K₂HPO₄, 0.5 g; MgSO₄, 0.025 g; H₂O, 1000 ml; pH 7.2–7.4).

2.2. Pathogenicity Analysis

The Pathogenicity of the *R. solanacearum* strain FJAT-1458 was determined with a leaf-cutting method by using four- to six-leaf stage plants of tissue culture seedling of

tomato (*Solanum lycopersicum* L. var. *goldstone* No. 1). The second, third and fourth leaves below the terminal bud of each seedling were cut about 1 cm length of wounds by a scissor. They were soaked in a bacterial suspension containing approximately 1×10⁷ cfu/ml for 20 minutes. The treated seedlings were incubated in a greenhouse at 30°C and 80% of relative humidity for 12 hours light/dark. SPA medium was used as negative control. Each treatment was replicated 10 times and the whole experiment was repeated twice. The disease incidence (wilt symptoms) of plants were monitored daily for 6 days.

2.3. Genomic DNA Preparation, Library Construction, Sequencing and Assembly

Bacterial cells were grown at 30°C overnight in SPA liquid medium. Genomic DNA was isolated and purified according to the manufacture’s instruction (Pacific Biosciences, Menlo Park, CA, USA). A 20-kb single-molecule real-time (SMRT) bell library was prepared with the SMRTbell template prep kit version 1.0 reagents (Pacific Biosciences, Menlo Park, CA, USA). The library was sequenced on a PacBio RS II sequencing platform using the C4 sequencing chemistry and P6 polymerase with 1 SMRT cells. The raw reads were filtered and assembled *de novo* following the Hierarchical Genome Assembly Process (HGAP) version 3.0 [20]. The polished assemblies were examined for circularity based on the presence of overlapping sequences at both ends of the contigs. Location of the overlapping sequence were determined using MUMmer version 3.0 [21].

2.4. Genome Annotation

The genome sequences were annotated using the NCBI prokaryotic annotation pipeline (<http://www.ncbi.nlm.nih.gov/genomes/static/Pipeline.html>). The circular map of the chromosome and plasmid were drawn by CGVIEW [22]. Prophage sequences were identified using PHASTER (<http://phaster.ca>) [23] and Insertion sequences were analyzed with ISEScan [24]. Functional annotation was based on BLAST searches against the NCBI RefSeq database, the Cluster of Orthologous Groups [25] and the Kyoto Encyclopedia of Genes and Genomes [26]. Protein domains were annotated using InterPro [27]. The classical secretory proteins were identified by SignalP (version 4.1, <http://www.cbs.dtu.dk/services/SignalP/>), and transmembrane helices were predicted by TMHMM (version 2.0, <http://www.cbs.dtu.dk/services/TMHMM/>).

2.5. Genomic Comparison

The complete genome sequences of FJAT-91, FQY 4, CQPS-1, CMR15, EP1, GMI1000, IBSBF1503, KACC10709, KACC10722, OE1-1, Po82, PS107, RS489, RS488, SEPPX05, UW163, UY031, YC40-M and YC45 were downloaded from the NCBI databases. The protein sequences of *egl*, *hrpB*, *mutS*, *pehA*, *recA*, *rpoA*, *rpoB* and *rpoC* genes were extracted and aligned using MUSCLE with default parameters [28]. The individual alignments were concatenated

successively to build the single super alignment. The best model for the alignment was estimated by MEGA software version 7.0 [29]. The phylogenetic tree was then constructed using Maximum Likelihood (ML) method in MEGA software version 7.0 [29]. The Jones-Taylor-Thornton (JTT) model assuming a discrete Gamma distribution (+G) with five rate categories was used for construction of a ML tree and the tree topology was evaluated by bootstrap analysis (1,000 replicates). Pairwise average nucleotide identity among these 19 strains were calculated with ANIm module of standalone version of JSpecies v1.2.1 with default parameters [30].

2.6. Nucleotide Sequence Deposition

The whole genome shotgun project has been deposited at DDBJ/EMBL/GenBank under the accession number CP016554 and CP016555 (BioProject ID PRJNA329182, and BioSample ID SAMN05392572).



Figure 1. Pathogenicity of *Ralstonia solanacearum* strains FJAT-1458 strains determined with a leaf-cutting method by using tomato seedling with 5-6 leaves after 6 days. (A) GM11000; (B) FJAT-1458; (C) control.

3.2. General Genomic Features and Genome Annotation of Strain FJAT-1458

Whole genome sequencing was carried out with single molecular real-time sequencing (SMRT) biotechnology on the PacBio RS II platform. The completed genome of *R. solanacearum* strain FJAT-1458 was 6.06 Mb with a GC content of 66.78%. It contained one circular chromosome (3.98 Mb with a GC content of 66.71%, Figure 2a) and one circular megaplasmid (2.08 Mb with a GC content of 66.92%, Figure 2b). A total of 5,166 protein-coding genes were

3. Results and Discussions

3.1. Pathogenicity Test of Strain FJAT-1458

The pathogenicity of *R. solanacearum* strain FJAT-1458 was determined with a leaf-cutting method by using tomato seedling with 5-6 leaves. Our results showed that strain FJAT-1458 is not able to cause wilt symptoms. However, the tomato seedlings began wilting at 4 days and reached to 58.33% incidence rate at 6 days after inoculated with *R. solanacearum* strain GM11000 (Figure 1). The pathogenicity of *R. solanacearum* strain FJAT-1458 against pepper and eggplant were also tested, and it is not able to cause wilt symptoms in either of these two plants as well. Our results suggested that strain FJAT-1458 is probably avirulent.

predicted (chromosome and megaplasmid encoded 3,633 and 1,533 genes, respectively). The FJAT-1458 genome contained 12 rRNA, 58 tRNA and 4 other non-coding RNAs. Of the 5,166 CDSs, 3,938 protein-coding genes can be assigned to 23 COG families. In addition, a total of 1,521 protein-coding genes had KEGG orthologs. 548 (10.61%) of protein-coding genes were predicted as classical secretory proteins with SignalP and 1,165 (22.55%) protein-coding genes have more than one transmembrane helix (Table 1).

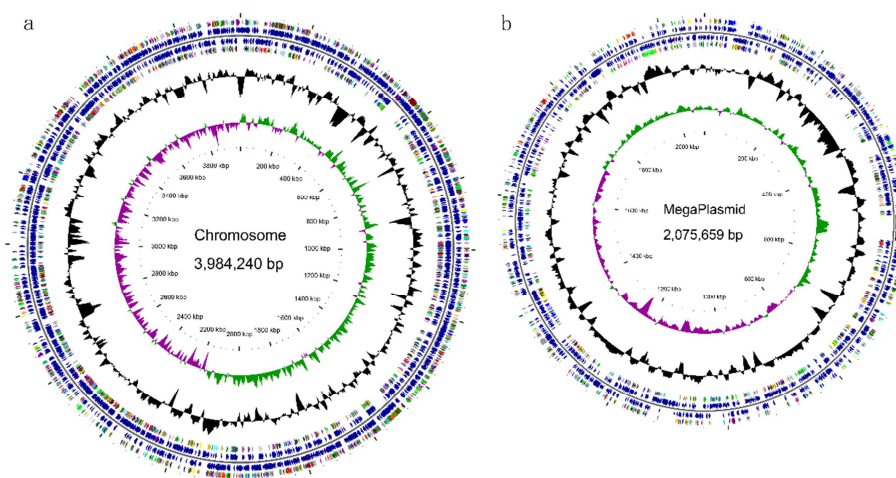


Figure 2. Circular genome map of *R. solanacearum* strain FJAT-1458. (A) chromosome of FJAT-1458; (B) megaplasmid of FJAT-1458. The distribution of the circle from inner to outer indicates, (1) circle 1: scale in kb; (2) circle 2: GC-skew (G-C/G+C ratio) using a 1 kb window with 100 bp step; (3) circle 3: GC-content using a 3 kb window with 100 bp step; (4) circle 4: COG assignments for predicted CDSs on the forward strand; (5) circle 5: COG assignments for predicted CDSs on the reverse strand.

Table 1. General genome features of the *Ralstonia solanacearum* strain FJAT-1458.

	Chromosome	Plasmid	Total
Genome Size (bp)	3,984,240	2,075,659	6,059,899
G+C content	66.71	66.92	66.78
Total genes	3,801	1,641	5,442
Protein coding genes	3,633	1,533	5,166
rRNA genes	9	3	12
tRNA genes	54	4	58
Other non-coding RNA genes	4	0	4
Pseudo genes	101	101	202
Hypothetical protein genes	898	473	1,371
Genes assigned to COGs	2,810	1,128	3,938
Genes assigned to GO function	2,027	790	2,817
Genes assigned to KEGG ontology	1,129	392	1,521
Genes with PFAM domains	2,996	1,206	4,202
Genes with assigned function	2,735	1,060	3,795
Genes with signal peptides	362	186	548
Genes with transmembrane helices	802	363	1,165

3.3. Prophages

A total of 7 intact, 1 questionable and 4 incomplete prophages were identified in the genome of *R. solanacearum* strain FJAT-1458 by PHASTER [23]. These prophages were designated as Prophage 1-12 (Supplementary Table A1). Among which, Prophage 1-10 were located on the chromosome and Prophage 11-12 were located on the mega-plasmid. Prophage size ranged between 5.17 kb and 58.9 kb in length and GC content ranged between 57.85% and 66.54%. The GC content of Prophage 1 (66.54%), Prophage 2 (66.19%), Prophage 5 (66.31%) and Prophage 6 (66.26%) were very close to the average GC content of the whole genome (66.78%), indicating that they might have been integrated into *R. solanacearum* genome long time ago.

Besides phage structural genes and IS elements, prophage carries large number of genes which provide new functions to the host (Supplementary Table A2). For example, we identified five DNA methyltransferase, three methylase, three

endonuclease and one exonuclease genes from these prophages, suggesting their role in DNA restriction and modification. We also identified two type III effector proteins and one type VI secretion system tip protein VgrG, which might contribute to virulence. Besides, we discovered a HicBA toxin-antitoxin II system in prophage 5, which encode a stable HicA toxin and a labile HicB antitoxin. TA systems are reported to be strongly correlated with physiological processes such as gene regulation, growth arrest, survival and apoptosis [31-34].

3.4. Comparative Genome Analysis

Phylogenetic relationships of *R. solanacearum* strain FJAT-1458 with other strains of *R. solanacearum* were assessed by performing Multilocus Sequence Analysis (MLSA) using eight genes (*egl*, *hrpB*, *mutS*, *pehA*, *recA*, *rpoA*, *rpoB* and *rpoC*). The result showed that strain FJAT-1458 belonged to phylotype I and was closest to strain YC-45 and SEPPX05 (Figure 3).

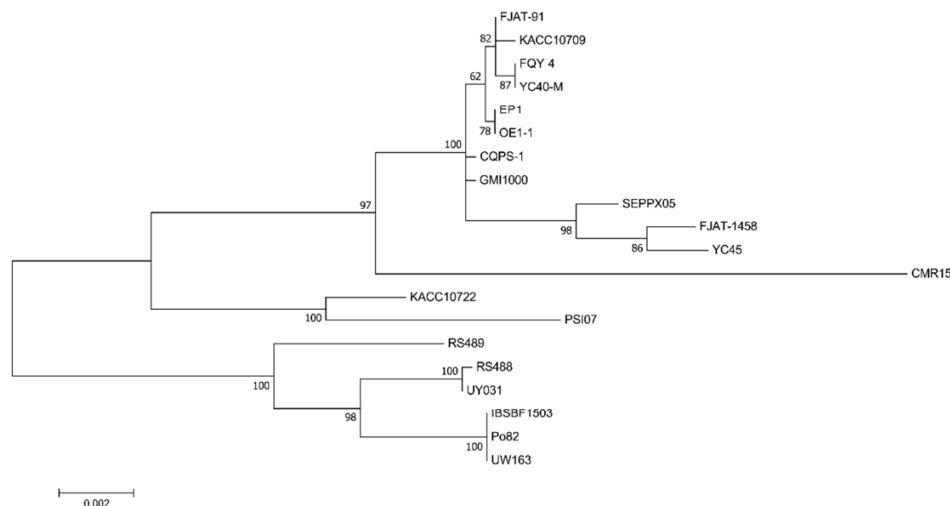


Figure 3. Phylogenetic reconstruction of *R. solanacearum* strain FJAT-1458 with other 19 of *R. solanacearum* strain. The phylogenetic tree was constructed using concatenated alignments of the marker genes *egl*, *hrpB*, *mutS*, *pehA*, *recA*, *rpoA*, *rpoB* and *rpoC*. The evolutionary history was inferred by using the Maximum Likelihood method base on the JTT model. A discrete Gamma distribution was used to model evolutionary rate differences among sites (5 categories (+G, parameter = 0.1000)). The rate variation model allowed for some sites to be evolutionarily invariable ([+I], 47.47% sites). Evolutionary analyses were conducted in MEGA 7.0 (Kumar S et al., 2016). The scale bar represents branch length measured in the number of substitutions per sites. Numbers at branch-points are percentages of 1000 bootstrap re-samplings that support the tree topology.

Based on average nucleotide identity (ANI) values, strains of *R. solanacearum* were grouped into three different genomespecies (Supplementary Table A3). The first group consists of strains from phylotype I and III. The second group includes phylotype II strains and the last group comprises strains from phylotype IV. ANI value is considered as one of the most robust measurements of genomic relatedness between strains and an ANI thresholds range (95~96%) correspond to $\geq 70\%$ DDH standard for species definition [35]. These ANI results indicate that these three genomespecies groups could be considered as separate species. Our results are consistent with previous reports [36, 37].

3.5. Genes Involved in Virulence

In this study, we showed that strain FJAT-1458 is avirulent to tomato, pepper and eggplant. To explore if avirulence of FJAT-1458 is due to the absence of key virulence factors, we created an inventory of 35 genes involved in virulence from GMI1000 [38], including exopolysaccharide (EPS) biosynthetic genes, cell wall degrading enzyme (CWDE) genes, response genes to the host defenses, key virulence regulator genes, chemotaxis genes, and genes involved in motility. Protein sequences predicted from the genome of strain FJAT-1458 were then searched against the database built from these virulence factors. Our results showed that these genes were well conserved between strain FJAT-1458 and GMI1000 (Supplementary Table A4), and the amino acid

sequence identities were more than 99%, except *phcB* and twitching motility gene *pilA*, whose identities were 86.02% and 93.49%, respectively.

3.6. T2SS

Type II Secretion System (T2SS) is one means by which Gram-negative pathogens secrete proteins into the extracellular milieu and/or host organisms [39]. In *R. solanacearum* strains, lots of proteins secreted in a Type-II-dependent manner which contribute to its virulence, and *R. solanacearum* strain with a defective type II secretion system (T2SSs) is weakly virulent [40]. Similar to strain GMI1000 [41], FJAT-1458 harbors three type II secretion systems (T2SS) (Figure 4). The first one is the orthodox system which contains 12 genes in the chromosome (from 355,322 to 367,621). This gene cluster is well conserved and shares a high sequence identity with strain GMI1000 (average amino acid sequence identity of 99.32%). The other two T2SSs are unorthodox systems. One includes seven core genes in the chromosome (ranging from 1,233,265 to 1,243,218) with four hypothetical genes inserted between *gspE* and *gspD* (Figure 4 b). The other possesses six core genes located in the mega-plasmid (from 1,835,267 to 1,844,143), with four hypothetical genes inserted between *gspD* and *gspE* (Figure 4 c). These two gene clusters are also conserved between strain GMI1000 and strain FJAT-1458 (average amino acid sequence identity of 98.68%).

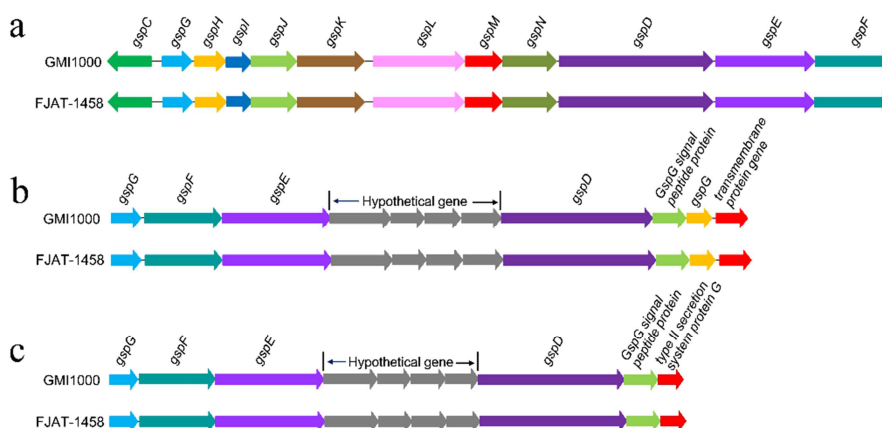


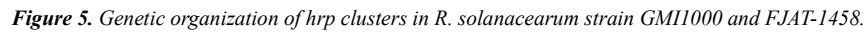
Figure 4. Genetic organization of T2SS gene clusters in strain FJAT-1458 and GMI1000. (A) The orthodox system of T2SS in the chromosome (from 355,322 to 367,621 bp); (B) one unorthodox system of T2SS in the chromosome (from 1,233,265 to 1,243,218 bp); (C) The other unorthodox system of T2SS in the megaplasmid (from 1,835,267 to 1,844,143 bp).

3.7. T3SS

The type III secretion system (T3SS) is widely spread in gram-negative bacteria, and is responsible for delivering bacterial proteins, termed effectors, from the bacterial cytosol directly into the interior of host cells [42]. These translocated proteins facilitate bacterial pathogenesis by specifically interfering with host cell signal transduction and other cellular processes [43]. The *hrp* gene cluster of T3SS is the key virulence determinant in *R. solanacearum*. In strain FJAT-1458, it is located on the megaplasmid and spans 29.655

kb (from 785,966 to 815,620), composed of 30 genes. Most of genes were well conserved between strain FJAT-1458 and GMI1000 (Figure 5), sharing amino acid sequence identity from 94.19% to 100.00%. One gene named *popC* was presumed to be pseudo due to internal stop codon.

A total of 68 T3es were identified in FJAT-1458 genome (Supplementary Table A5). Among which, 62 (91.18%) of them were also present in the strain GMI1000. Six T3es were present in strain FJAT-1458 but absent in strain GMI1000, while 12 T3es were absent in strain FJAT1458 but were present in strain GMI1000.



The Type IV Secretion System (T4SS) plays diverse important roles in virulence and adaption. In strain GMI1000, the T4SS gene cluster is comprised of 17 genes (*RSc2574-RSc2588*, *RSp0179*, and *RSp1521*) [41]. No experimental evidence is yet available in support of a role for these genes as a “fitness island” or an “ecological island” [44]. These 17 T4SS genes were searched against the genome of strain FJAT-1458, and none of them were identified in this genome.

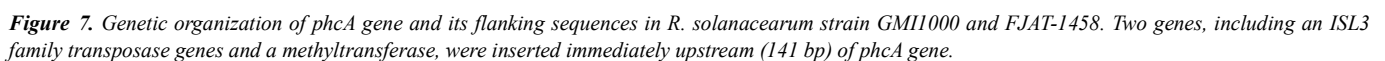
The type VI secretion system (T6SS) is a complex and widespread gram-negative bacterial export pathway with the

[illegible]

Figure 6. Genetic organization of T6SS system in *R. solanacearum* strain GM1000 and FJAT-1458.

Comparison of virulence factors between strain GMI1000 and strain FJAT-1458 revealed that most of them are well conserved between them, and only small portion of virulence factors are distinct. These distinct virulence factors might lead to weakened virulence instead of loss of virulence. Previous study revealed that the LysR family transcriptional regulator PhcA plays a central role which regulates directly and indirectly many of those virulence genes [12] and inactivation of *phcA* gene resulted in loss of virulence [14-16]. A previous genetic study carried out with strain AW1 showed that spontaneous PC can be attributed to insertions with *phcA* gene (2-bp, 200-bp or 1-kb insertions) [14]. Another independent research with three spontaneous PC mutation strains of ACH0158 also showed that inactivation of *phcA* gene (an

insertion of *ISRso4*, a 132bp-deletion and a 2-bp insertion) results in loss of virulence [16]. Thus, we carefully examined the *phcA* gene and its flanking sequence. We didn't find any insertion sequence in *phcA* gene and it is well conserved between strain GMI1000 and strain FJAT-1458 (coverage 100.00%, identity 99.71%). However, we did find two genes, including a methyltransferase and an ISL3 family transposase genes, inserted immediately upstream (141 bp) of *phcA* gene (Figure 7). This insertion sequence might suppress the expression of *phcA* gene as it is just located in the promoter region of *phcA* gene. The low levels of functional PhcA could not be able to activate the transcription of its downstream genes associated with the virulence of the pathogen [47], which finally resulted in avirulence of FJAT-1458. Further experiments (such as transcriptome analysis and genetic compensation experiment) are still required to confirm.



4. Conclusions

An avirulent *R. solanacearum* strain named FJAT-1458 was isolated from living tomato vessel and it showed no toxicity to tomato, pepper and eggplant. Comparative genome analyses between GMI1000 and FJAT-1458 revealed that a fragment, containing a methyltransferase and an ISL3 family transposase genes, was inserted immediately upstream (141 bp) of *phcA* gene, which assumed to be responsible for avirulence of FJAT-1458. It is suggested that strain FJAT-1458 was originated from a wild-type pathogenic strain through an accident phenotype conversion, which is like those when cultured under experimental conditions. Our study provides new insight into the evolution of virulence in *R. solanacearum*

strain under natural environment.

Author Contributions

CD, LB and ZH conceived and designed the experiments. CD, LY, CY, CJ performed the experiments. CD, CJ and WJ generated and analyzed the data. CD wrote the paper.

Acknowledgements

This work was funded by the Fujian Natural Science Foundation (2017J01049).

Appendix

Table A1. Whole genome average nucleotide identity (ANI) analysis of 20 strains from *R. solanacearum* species.

		FJAT-1458	KACC 10709	FJAT-91	FQY_4	YC40-M	OE1-1	EP1	YC45	GMI1000	SEPPX05
		I	I	I	I	I	I	I	I	I	I
FJAT-1458	I	-	99.40	99.29	98.99	98.88	98.71	98.58	98.58	98.57	98.60
KACC10709	I	99.36	-	99.38	99.15	99.12	98.88	98.83	98.81	98.77	98.85
FJAT-91	I	99.28	99.41	-	99.01	98.91	98.77	98.65	98.65	98.65	98.68
FQY_4	I	98.92	99.14	98.97	-	99.75	98.73	98.68	98.72	98.66	98.80
YC40-M	I	98.84	99.14	98.88	99.77	-	98.66	98.57	98.63	98.57	98.68
OE1-1	I	98.66	98.89	98.74	98.76	98.68	-	99.59	98.68	98.72	98.75
EP1	I	98.58	98.85	98.66	98.72	98.60	99.62	-	98.60	98.67	98.66
YC45	I	98.57	98.83	98.63	98.76	98.66	98.70	98.59	-	98.77	98.77
GMI1000	I	98.57	98.81	98.64	98.72	98.61	98.74	98.65	98.80	-	98.79
SEPPX05	I	98.57	98.88	98.68	98.83	98.72	98.76	98.64	98.75	98.76	-
CQPS-1	I	98.56	98.80	98.62	98.71	98.64	99.06	98.97	98.75	98.77	98.76
CMR15	III	95.82	96.04	95.89	95.97	95.94	95.91	95.78	95.88	95.89	95.93
KACC10722	IV	92.84	92.95	92.87	92.82	92.94	92.85	92.83	92.77	92.77	92.84
PS107	IV	92.73	92.80	92.74	92.72	92.82	92.74	92.70	92.72	92.73	92.73
UY031	II	91.53	91.63	91.55	91.58	91.59	91.58	91.52	91.60	91.52	91.62
RS488	II	91.48	91.58	91.49	91.52	91.54	91.53	91.47	91.53	91.47	91.56
Po82	II	91.47	91.65	91.49	91.51	91.50	91.53	91.48	91.55	91.60	91.53
IBSBF1503	II	91.47	91.65	91.49	91.51	91.51	91.53	91.47	91.55	91.59	91.52
UW163	II	91.46	91.63	91.47	91.51	91.51	91.53	91.48	91.54	91.59	91.53
RS489	II	91.42	91.52	91.43	91.46	91.47	91.46	91.39	91.49	91.42	91.50

Table A1. Continued.

		CQPS-1	CMR15	KACC 10722	PS107	UY031	RS488	Po82	IBSBF 1503	UW163	RS489
		I	III	IV	IV	II	II	II	II	II	II
FJAT-1458	I	98.50	95.83	92.84	92.72	91.53	91.47	91.48	91.47	91.47	91.41
KACC10709	I	98.76	96.07	92.95	92.79	91.62	91.55	91.65	91.64	91.62	91.51
FJAT-91	I	98.52	95.88	92.87	92.72	91.55	91.48	91.49	91.48	91.48	91.43
FQY_4	I	98.65	95.97	92.81	92.71	91.57	91.50	91.49	91.49	91.50	91.45
YC40-M	I	98.57	95.94	92.92	92.80	91.58	91.51	91.48	91.49	91.50	91.46
OE1-1	I	98.98	95.93	92.85	92.73	91.58	91.52	91.52	91.53	91.52	91.45
EP1	I	98.92	95.79	92.86	92.70	91.52	91.45	91.49	91.47	91.48	91.38
YC45	I	98.67	95.89	92.77	92.73	91.59	91.53	91.55	91.54	91.54	91.48
GMI1000	I	98.67	95.92	92.77	92.74	91.52	91.47	91.59	91.57	91.58	91.41
SEPPX05	I	98.66	95.95	92.85	92.73	91.62	91.56	91.52	91.51	91.51	91.49
CQPS-1	I	-	95.92	92.84	92.75	91.55	91.49	91.58	91.57	91.55	91.43
CMR15	III	95.82	-	92.52	92.45	91.52	91.46	91.55	91.55	91.54	91.38
KACC10722	IV	92.86	92.52	-	98.32	92.23	92.17	92.18	92.14	92.15	92.05
PS107	IV	92.75	92.45	98.32	-	92.16	92.09	92.08	92.00	92.05	92.01
UY031	II	91.51	91.52	92.24	92.18	-	99.83	97.43	97.40	97.41	97.27
RS488	II	91.46	91.46	92.18	92.11	99.83	-	97.34	97.32	97.33	97.20
Po82	II	91.51	91.55	92.19	92.10	97.43	97.35	-	99.74	99.73	96.38

		CQPS-1	CMR15	KACC 10722	PS107	UY031	RS488	Po82	IBSBF 1503	UW163	RS489
		I	III	IV	IV	II	II	II	II	II	II
IBSBF1503	II	91.49	91.55	92.15	92.01	97.40	97.33	99.72	-	99.70	96.36
UW163	II	91.49	91.54	92.17	92.07	97.42	97.34	99.75	99.74	-	96.38
RS489	II	91.39	91.39	92.07	92.03	97.26	97.20	96.38	96.35	96.36	-

Table A2. Summary of prophages predicted in FJAT-1458.

ID	Location	Completeness	Start	End	Length	Total Protein numbers	GC Content	ATT Sites
Prophage 1	Chromosome	questionable(90)	220332	236365	16034	21	66.54%	No
Prophage 2	Chromosome	intact(150)	426995	463041	36047	49	66.19%	Yes
Prophage 3	Chromosome	intact(122)	1622955	1666443	43489	48	64.49%	Yes
Prophage 4	Chromosome	intact(150)	1875020	1933963	58944	53	64.61%	Yes
Prophage 5	Chromosome	intact(150)	1938002	1958812	20811	26	66.31%	No
Prophage 6	Chromosome	intact(133)	2168497	2190188	21692	17	64.90%	Yes
Prophage 7	Chromosome	intact(97)	2596449	2641654	45206	41	63.96%	Yes
Prophage 8	Chromosome	intact(150)	2726121	2771275	45155	45	59.20%	No
Prophage 9	Chromosome	incomplete(40)	2957099	2976375	19277	18	66.26%	No
Prophage 10	Chromosome	incomplete(40)	3037730	3052587	14858	10	64.67%	No
Prophage 11	Megaplasmid	incomplete(50)	337007	345420	8414	11	60.78%	No
Prophage 12	Megaplasmid	incomplete(60)	1661567	1666733	5167	8	57.85%	No
Total					321513	347		

Table A3. Functional annotation of genes predicted in prophages of FJAT-1458.

ID	Location	Start	End	Strand	Annotation
1	Chromosome	220332	221732	+	DNA modification methylase
2	Chromosome	221729	222949	+	DNA methylase N-4
3	Chromosome	223129	224094	-	IS5-like element IS1405 family transposase
4	Chromosome	224170	224535	-	hypothetical protein
5	Chromosome	224703	224897	+	hypothetical protein
6	Chromosome	225059	225427	+	hypothetical protein
7	Chromosome	225582	225770	-	hypothetical protein
8	Chromosome	225892	226386	-	DUF3489 domain-containing protein
9	Chromosome	226476	226745	+	hypothetical protein
10	Chromosome	226842	227378	+	elements of external origin
11	Chromosome	227378	229345	+	phage terminase large subunit family protein
12	Chromosome	229389	229898	+	capsid-related protein
13	Chromosome	229909	230301	+	tail fiber
14	Chromosome	230302	230523	+	head-tail connector
15	Chromosome	230523	232049	+	lambda-like phage portal protein
16	Chromosome	232059	233309	+	putative head maturation protease
17	Chromosome	233319	233696	+	head decoration protein D
18	Chromosome	233705	234709	+	minor capsid protein E
19	Chromosome	234712	235014	+	hypothetical protein
20	Chromosome	235020	235466	+	hypothetical protein
21	Chromosome	235592	236365	+	hypothetical protein

Table A4. Comparative analysis of known and candidate virulence factors (except for Type III effectors) between strain FJAT-1458 and GM11000.

Virulence_Category	GM11000			Length	Start	End
	Locus_tag	Symbl	Description			
EPS biosynthetic genes	RSp1014	epsF	EPS I polysaccharide export inner membrane protein	418	1	418
	RSp1015	epsE	EPS I polysaccharide export inner membrane protein	436	1	436
	RSp1016	epsD	NDP-N-acetyl-D-galactosaminuronic acid dehydrogenase	423	1	423
	RSp1017	epsC	UDP-N-acetylglucosamine 2-epimerase	375	1	375
	RSp1018	epsB	Tyrosine-protein kinase epsB (EPS I polysaccharide export protein epsB)	751	1	751
	RSp1019	epsP	Low molecular weight protein-tyrosine-phosphatase epsP	145	1	145
	RSp1020	epsA	EPS I polysaccharide export outer membrane protein	381	1	381
	RSp0338	epsR	Negative regulator of exopolysaccharide production	222	1	222
Cell Wall Degrading Enzymes (CWDE)	RSc1756	pehB	Exo-poly-galacturonidase	702	1	702
	RSp0833	pehC	Polygalacturonase	680	1	680
	RSp0162	egl	endoglucanase	436	1	436
	RSc0319	plcN	non hemolytic phospholipase C	700	1	700
Response to host defenses	RSp1581	katE	catalase hydroperoxidase HpiI oxidoreductase	509	1	509
	RSc2690	oxyR	Hydrogen peroxide-inducible gene activator	314	1	314
	RSp0283	dinF	DNA-damage-inducible SOS response protein	457	1	457

Virulence_Category	GMI1000					
	Locus_tag	Symbl	Description	Length	Start	End
Key virulence regulators	RSc0011	acrA	component of acridine efflux pump, multidrug efflux system	398	1	398
	RSc0010	acrB	component of acridine efflux pump, multidrug efflux system	1049	1	1049
	RSc2748	phcA	transcriptional regulator, LysR family	347	1	347
	RSc2735	phcB	regulatory protein, SAM-dependent methyltransferase domain	467	1	465
	RSc0289	vsrA	Transmembrane sensor kinase	474	1	474
	RSc0292	vsrD	response regulator, LuxR family	210	1	210
	RSc2456	vsrB		611	1	611
	RSc2455	vsrC		221	1	221
	RSp1003	xpsR		306	1	306
	RSc2808	pehS	sensor histidine kinase transcription regulator	682	1	682
Chemotaxis	RSc2807	pehR	response regulator receiver, FIS type, sigma 54 interacting region	560	1	560
	RSc3286	solI		204	1	204
	RSc3287	solR	Transcriptional activator	236	1	236
Swimming motility	RSp1408	cheA		726	1	726
	RSp1407	cheW	chemotaxis protein; regulation	163	1	163
Twitching motility	RSp0382	fliC		273	1	273
	RSp0340	flgM		106	1	106
	RSc0558	pilA		168	1	168
	RSc2972	pilP		181	1	181

Table A4. Continued.

Virulence_Category	FJAT-1458					
	Locus_Tag	Length	Start	End	Alignment_Length	Identity
EPS biosynthetic genes	BCR16_RS23200	418	1	418	418	100.00
	BCR16_RS23205	436	1	436	436	99.77
	BCR16_RS23210	423	1	423	423	100.00
	BCR16_RS23215	375	1	375	375	99.73
	BCR16_RS23220	751	1	751	751	99.87
	BCR16_RS23225	145	1	145	145	100.00
	BCR16_RS23230	381	1	381	381	100.00
Cell Wall Degrading Enzymes (CWDE)	BCR16_RS12005	222	1	222	222	100.00
	BCR16_RS09865	702	1	702	702	99.00
	BCR16_RS22545	680	1	680	680	99.56
	BCR16_RS26440	436	1	436	436	99.31
Response to host defenses	BCR16_RS17325	700	1	700	700	99.86
	BCR16_RS25405	509	1	509	509	99.80
	BCR16_RS04445	314	1	314	314	100.00
	BCR16_RS27070	457	1	457	457	100.00
	BCR16_RS18965	398	1	398	398	99.25
	BCR16_RS18970	1049	1	1049	1049	100.00
	BCR16_RS04065	347	1	347	347	99.71
Key virulence regulators	BCR16_RS04130	468	1	465	465	86.02
	BCR16_RS17475	474	1	474	474	100.00
	BCR16_RS17460	210	1	210	210	100.00
	BCR16_RS05275	611	1	611	611	100.00
	BCR16_RS05280	221	1	221	221	100.00
	BCR16_RS23145	306	1	306	306	100.00
	BCR16_RS03755	682	1	682	682	99.85
Chemotaxis	BCR16_RS03760	560	1	560	560	99.82
	BCR16_RS00745	204	1	204	204	99.51
	BCR16_RS00740	236	1	236	236	99.58
	BCR16_RS24585	726	1	726	726	100.00
	BCR16_RS24580	163	1	163	163	100.00
	BCR16_RS19420	273	1	273	273	100.00
	BCR16_RS19210	106	1	106	106	100.00
Twitching motility	BCR16_RS16060	169	1	169	169	93.49
	BCR16_RS02890	181	1	181	181	100.00

Table A5. Comparative analysis of Type III effectors between strain FJAT-1458 and GMI1000.

Virulence_Category	GMI1000					
	Locus_tag	Symbl	Description	Length	Start	End
Type III effectors & putative effectors	RSp0914	GALA1	LRR F-box protein, Interaction with SKP1-like proteins	661	1	661
	RSp0672	GALA2	LRR F-box protein	1035	55	1035
	RSp0028	GALA3	LRR F-box protein, Interaction with SKP1-like proteins	518	1	518

Virulence_Category	GMI1000			Length	Start	End
	Locus_tag	Symb1	Description			
	RSc1800	GALA4	LRR F-box protein	401	1	401
	Rsc1801	GALA5	LRR F-box protein, Interaction with SKP1-like proteins	522	1	522
	RSc1356	GALA6	LRR F-box protein, Interaction with SKP1-like proteins	620	1	620
	Rsc1357	GALA7	LRR F-box protein, Host specificity factor on medicago truncatula	647	1	647
	RSc3401	SKWP1	Heat/armadillo-related repeats	2353	1	2353
	RSp1374	SKWP2	Heat/armadillo-related repeats	2483	1	2467
	RSp0930	SKWP3	Heat/armadillo-related repeats	2208	1	2208
	RSc1839	SKWP4	Heat/armadillo-related repeats	2497	1	2497
	RSp0296	SKWP5	Heat/armadillo-related repeats	2338	1	2338
	RSc2130	SKWP6	Heat/armadillo-related repeats	721	1	721
	RSc1386	HLK1		765	1	765
	RSp0215	HLK2		754	1	754
	RSp0160	HLK3		719	1	719
	Rsc1349	SspH1 family		685	1	685
	Rsc0245	ripB	Nucleoside hydrolase domain	492	1	492
	Rsc2775	popW	Harpin with pectate lyase domain	380	1	380
	RSp0304	AvrPphD family	Required for full virulence on tomato	643	1	643
	RSp0323	HopG1 family		451	1	451
	Rsp0732	HopAV1 family	Coiled-coil domain	830	1	830
	RSp0875	popC	Leucine Rich repeats			
	Rsp1281	HopR1 family		1742	1	1742
	RSc0826	PopP1 (YopJ family)	S/T acetyltransferase domain, avirulence factor on some petunia lines	368	1	368
	Rsc1815	AvrBs3 family	35AA repeats units			
	RSc3212	RipT (YopT family)	Cysteine protease domain	321	1	321
	Rsc3290	HopH1 family				
	Rsc3369	AvrPphE family		425	1	425
	RSp0572	HopH1 family		218	36	218
	RSp0822	AvrPphF family		288	1	288
	Rsp1239	-		943	107	943
	Rsp1277	HopAA1 family		361	1	361
	Rsc0041	-		430	1	430
	RSc0608	AvrA	Avirulence factor on Nicotiana species			
	RSc1475	-		584	1	584
	RSc3272	-		154	1	154
	Rsp0731	-		557	59	557
	Rsp0845	-		1390	1	1390
	Rsp0876	popB		174	1	174
	Rsp0877	popA	Harpin, Formation of ion-conducting pores	344	1	344
	Rsp0882	-		299	1	299
	RSp1022	-		346	1	346
	RSp1236	-		540	1	540
	RSp0099	AWR2, RipA	Required for full virulence on tomato	1127	1	1127
	RSp0846	AWR3		1193	1	1193
	RSp0847	AWR4		1330	1	1330
	RSp1024	AWR5		1146	1	1146
	RSc2139	AWR1		1063	1	1063
	Rsp0257	-	Ankyrin repeats	277	1	277
	RSc0321	-				
	RSc0824	-		98	1	98
	RSc0868	PopP2	Functionnal NLS, S/T acetyltransferase domain, avirulence factor on Arabidopsis	488	1	488
	RSc0895	-		96	1	96
	RSc1723	-				
	RSc2101	-		306	1	306
	RSc2359	-		739	1	739
	RSc3174	-				
	RSp0193	-	Pentatricopeptide repeat domain	1373	1	1359
	RSp0213	-				
	Rsp0216	-	S/T kinase domain			
	RSp0218	-	oxydoreductase domain	311	1	307
	RSp0885	-		703	1	703
	RSp1031	-	Coiled-coil domain	1310	1	1310
	RSp1212	-				
	RSp1384	-		878	1	878

Virulence_Category	GMI1000				
	Locus_tag	Symbl	Description	Length	Start End
	RSp1388	-		461	83 461
	RSp1460	-		274	1 274
	RSp1475	-		369	1 369
	RSp1582	-			
	RSp1601	-		248	1 248
	RSc2132	-			
	RSp0879	-		487	1 487
	RSp1130	-	Nudix hydrolase domain	474	1 474

Table A5. Continued.

Virulence_Category	FJAT-1458				Alignment_Length	Identity
	Locus_Tag	Length	Start	End		
Type III effectors & putative effectors	BCR16_RS22160	589	1	589	661	88.35
	BCR16_RS21450	981	1	981	981	97.76
	BCR16_RS26065	522	1	522	522	95.98
	BCR16_RS10075	401	1	401	401	99.25
	BCR16_RS10080	522	1	522	522	98.47
	BCR16_RS11095	620	1	620	620	97.26
	BCR16_RS11090	647	1	647	647	96.91
	BCR16_RS00145	2353	1	2353	2353	99.19
	BCR16_RS24375	2512	1	2469	2469	98.95
	BCR16_RS22045	2208	1	2208	2208	98.60
	BCR16_RS10265	2495	1	2495	2497	98.00
	BCR16_RS27125	2338	1	2338	2338	99.02
	BCR16_RS06900	721	1	721	721	99.03
	BCR16_RS10945	765	1	765	765	98.69
	BCR16_RS26710	742	1	742	754	96.42
	BCR16_RS26430	719	1	719	719	98.89
	BCR16_RS11130	685	1	685	685	97.52
	BCR16_RS17735	492	1	492	492	99.39
	BCR16_RS03925	380	1	380	380	99.47
	BCR16_RS27145	641	1	641	643	96.73
	BCR16_RS19125	501	51	501	451	98.67
	BCR16_RS23055	830	1	830	830	99.52
	BCR16_RS20755	1742	1	1742	1742	99.25
	BCR16_RS14705	368	1	368	368	95.11
	BCR16_RS14580	321	1	321	321	99.69
	BCR16_RS00305	425	1	425	425	99.06
	BCR16_RS20560	183	1	183	183	79.23
	BCR16_RS22600	292	1	292	292	95.55
	BCR16_RS20960	837	1	837	837	98.69
	BCR16_RS20775	361	1	361	361	99.17
	BCR16_RS18800	430	1	430	430	99.07
	BCR16_RS10490	584	1	584	584	98.97
	BCR16_RS00820	154	1	154	154	99.35
	BCR16_RS23060	499	1	499	499	99.60
	BCR16_RS22480	1390	1	1390	1390	99.50
	BCR16_RS22325	174	1	174	174	98.85
	BCR16_RS22320	330	1	330	344	94.19
	BCR16_RS22295	299	1	299	299	100.00
	BCR16_RS23240	411	71	411	346	95.38
	BCR16_RS24280	540	1	540	540	98.33
	BCR16_RS26190	1126	1	1126	1127	99.47
	BCR16_RS22475	1189	1	1189	1193	98.41
	BCR16_RS22470	1333	1	1333	1334	98.58
	BCR16_RS23255	1146	1	1146	1146	99.21
	BCR16_RS06850	1067	1	1067	1067	98.59
	BCR16_RS26945	280	1	280	280	98.93
	BCR16_RS14710	98	1	98	98	100.00
	BCR16_RS01205	488	1	488	488	98.57
	BCR16_RS14380	96	1	96	96	100.00
	BCR16_RS07055	306	1	306	306	99.35
	BCR16_RS05785	739	1	739	739	99.73
	BCR16_RS26610	1337	1	1323	1360	94.63
	BCR16_RS26725	866	1	307	307	98.37

Virulence_Category	FJAT-1458				Alignment_Length	Identity
	Locus_Tag	Length	Start	End		
	BCR16_RS22280	703	1	703	703	98.44
	BCR16_RS23295	1306	1	1306	1310	98.70
	BCR16_RS24465	878	1	878	878	98.86
	BCR16_RS24485	379	1	379	379	97.63
	BCR16_RS24825	274	1	274	274	98.54
	BCR16_RS24910	369	1	369	369	97.56
	BCR16_RS25490	248	1	248	248	97.58
	BCR16_RS22310	481	1	481	487	96.51
	BCR16_RS23795	474	1	474	474	97.05
	BCR16_RS06885					
	BCR16_RS06895					
	BCR16_RS10280					
	BCR16_RS17315					
	BCR16_RS22120					
	BCR16_RS25410					

References

- [1] Denny TP: Plant pathogenic *Ralstonia* species. In *plant-Associated Bacteria*, ed. SS Gnanamanickam: Dordrecht, The Netherlands: Springer; 2006.
- [2] Genin S: Molecular traits controlling host range and adaptation to plants in *Ralstonia solanacearum*. *The New phytologist* 2010, 187 (4): 920-928.
- [3] van Overbeek LS, Bergervoet JH, Jacobs FH, van Elsas JD: The Low-Temperature-Induced Viable-But-Nonculturable State Affects the Virulence of *Ralstonia solanacearum* Biovar 2. *Phytopathology* 2004, 94 (5): 463-469.
- [4] Hayward AC: Biology and epidemiology of bacterial wilt caused by *pseudomonas solanacearum*. *Annual review of phytopathology* 1991, 29: 65-87.
- [5] Yuliar, Nion YA, Toyota K: Recent trends in control methods for bacterial wilt diseases caused by *Ralstonia solanacearum*. *Microbes and environments / JSME* 2015, 30 (1): 1-11.
- [6] Lopes MM, G. BE: Potato bacterial wilt management: new prospects for an old problem, in *Bacterial Wilt Disease and the Ralstonia solanacearum Species Complex* edn: Saint Paul, MN: APS Press; 2005.
- [7] Saddler GS: Management of bacterial wilt disease, in *Bacterial Wilt Disease and the Ralstonia solanacearum Species Complex* edn: Saint Paul, MN: APS press; 2005.
- [8] Zheng XA, Li XJ, Wang BS, Cheng D, Li YP, Li WH, Huang MH, Tan XD, Zhao GZ, Song BT, Macho AP, Chen HL, Xie CH: A systematic screen of conserved *Ralstonia solanacearum* effectors reveals the role of RipAB, a nuclear-localized effector that suppresses immune responses in potato. *Molecular Plant Pathology*, 2019, 20 (4), 547-561.
- [9] Tampakaki AP, Skandalis N, Gazi AD, Bastaki MN, Sarris PF, Charova SN, Kokkinidis M, Panopoulos NJ: Playing the "Harp": evolution of our understanding of hrp/hrc genes. *Annual review of phytopathology* 2010, 48: 347-370.
- [10] Hayashi K, Kai K, Mori Y, Ishikawa S, Ujita Y, Ohnishi K, Kiba A, Hikichi Y: Contribution of a lectin, LecM, to the quorum sensing signalling pathway of *Ralstonia solanacearum* strain OE1-1. *Molecular Plant Pathology*, 2019, 20 (3), 334-345.
- [11] Genin S, Denny TP: Pathogenomics of the *Ralstonia solanacearum* species complex. *Annual review of phytopathology* 2012, 50: 67-89.
- [12] Peeters N, Guidot A, Vailleau F, Valls M: *Ralstonia solanacearum*, a widespread bacterial plant pathogen in the post-genomic era. *Molecular plant pathology* 2013, 14 (7): 651-662.
- [13] Mori T, Fujiyoshi T, Inada T, Matsusaki H, Ogawa K, Matsuzoe N: Phenotypic Conversion of *Ralstonia solanacearum* in Susceptible and Resistant Solanum Plants. *Environment Control in Biology* 2011, 49: 165-176.
- [14] Zhang Y, Li JM, Zhang WQ, Shi HL, Luo F, Hikich Y, Shi XJ, Ohnishi K: A putative LysR - type transcriptional regulator PrhO positively regulates the type III secretion system and contributes to the virulence of *Ralstonia solanacearum*. *Molecular Plant Pathology*, 2018, 19 (8): 1808-1819.
- [15] Khokhani D, Lowe-Power TM, Tran TM, Allen C: A Single Regulator Mediates Strategic Switching between Attachment/Spread and Growth/Virulence in the Plant Pathogen *Ralstonia solanacearum*. *mBio* , 2017 , 8 (5): e00895-17.
- [16] Jeong EL, Timmis JN: Novel insertion sequence elements associated with genetic heterogeneity and phenotype conversion in *Ralstonia solanacearum*. *Journal of bacteriology* 2000, 182 (16): 4673-4676.
- [17] Poussier S, Thoquet P, Trigalet-Demery D, Barthet S, Meyer D, Arlat M, Trigalet A: Host plant-dependent phenotypic reversion of *Ralstonia solanacearum* from non-pathogenic to pathogenic forms via alterations in the phcA gene. *Molecular microbiology* 2003, 49 (4): 991-1003.
- [18] Zheng X, Zhu Y, Liu B, Yu Q, Lin N: Rapid differentiation of *Ralstonia solanacearum* avirulent and virulent strains by cell fractioning of an isolate using high performance liquid chromatography. *Microbial pathogenesis* 2016, 90: 84-92.
- [19] Kelman A, Hruschka J: The role of motility and aerotaxis in the selective increase of avirulent bacteria in still broth cultures of *Pseudomonas solanacearum*. *Journal of general microbiology* 1973, 76 (1): 177-188.
- [20] Chin CS, Alexander DH, Marks P, Klammer AA, Drake J, Heiner C, Clum A, Copeland A, Huddleston J, Eichler EE *et al*: Nonhybrid, finished microbial genome assemblies from long-read SMRT sequencing data. *Nature methods* 2013, 10 (6): 563-569.

- [21] Kurtz S, Phillippy A, Delcher AL, Smoot M, Shumway M, Antonescu C, Salzberg SL: Versatile and open software for comparing large genomes. *Genome biology* 2004, 5 (2): R12.
- [22] Stothard P, Wishart DS: Circular genome visualization and exploration using CGView. *Bioinformatics* 2005, 21 (4): 537-539.
- [23] Arndt D, Grant JR, Marcu A, Sajed T, Pon A, Liang Y, Wishart DS: PHASTER: a better, faster version of the PHAST phage search tool. *Nucleic acids research* 2016, 44 (W1): W16-21.
- [24] Xie Z, Tang H: ISEScan: automated identification of insertion sequence elements in prokaryotic genomes. *Bioinformatics* 2017, 33 (21): 3340-3347.
- [25] Tatusov RL, Fedorova ND, Jackson JD, Jacobs AR, Kiryutin B, Koonin EV, Krylov DM, Mazumder R, Mekhedov SL, Nikolskaya AN *et al*: The COG database: an updated version includes eukaryotes. *BMC bioinformatics* 2003, 4: 41.
- [26] Moriya Y, Itoh M, Okuda S, Yoshizawa AC, Kanehisa M: KAAS: an automatic genome annotation and pathway reconstruction server. *Nucleic acids research* 2007, 35 (Web Server issue): W182-185.
- [27] Jones P, Binns D, Chang HY, Fraser M, Li W, McAnulla C, McWilliam H, Maslen J, Mitchell A, Nuka G *et al*: InterProScan 5: genome-scale protein function classification. *Bioinformatics* 2014, 30 (9): 1236-1240.
- [28] Edgar RC: MUSCLE: multiple sequence alignment with high accuracy and high throughput. *Nucleic acids research* 2004, 32 (5): 1792-1797.
- [29] Kumar S, Stecher G, Tamura K: MEGA7: Molecular Evolutionary Genetics Analysis Version 7.0 for Bigger Datasets. *Molecular biology and evolution* 2016, 33 (7): 1870-1874.
- [30] Richter M, Rossello-Mora R: Shifting the genomic gold standard for the prokaryotic species definition. *Proceedings of the National Academy of Sciences of the United States of America* 2009, 106 (45): 19126-19131.
- [31] Gerdes K, Christensen SK, Lobner-Olesen A: Prokaryotic toxin-antitoxin stress response loci. *Nature reviews Microbiology* 2005, 3 (5): 371-382.
- [32] Van Melder L: Toxin-antitoxin systems: why so many, what for? *Current opinion in microbiology* 2010, 13 (6): 781-785.
- [33] Hayes F, Van Melder L: Toxins-antitoxins: diversity, evolution and function. *Critical reviews in biochemistry and molecular biology* 2011, 46 (5): 386-408.
- [34] Buts L, Lah J, Dao-Thi MH, Wyns L, Loris R: Toxin-antitoxin modules as bacterial metabolic stress managers. *Trends in biochemical sciences* 2005, 30 (12): 672-679.
- [35] Goris J, Konstantinidis KT, Klappenbach JA, Coenye T, Vandamme P, Tiedje JM: DNA-DNA hybridization values and their relationship to whole-genome sequence similarities. *International journal of systematic and evolutionary microbiology* 2007, 57 (Pt 1): 81-91.
- [36] Prior P, Ailloud F, Dalsing BL, Remenant B, Sanchez B, Allen C: Genomic and proteomic evidence supporting the division of the plant pathogen *Ralstonia solanacearum* into three species. *BMC genomics* 2016, 17: 90.
- [37] Remenant B, de Cambiaire JC, Cellier G, Jacobs JM, Mangelot S, Barbe V, Lajus A, Vallenet D, Medigue C, Fegan M *et al*: *Ralstonia syzygii*, the Blood Disease Bacterium and some Asian *R. solanacearum* strains form a single genomic species despite divergent lifestyles. *PloS one* 2011, 6 (9): e24356.
- [38] Remenant B, Coupat-Goutaland B, Guidot A, Cellier G, Wicker E, Allen C, Fegan M, Pruvost O, Elbaz M, Calteau A *et al*: Genomes of three tomato pathogens within the *Ralstonia solanacearum* species complex reveal significant evolutionary divergence. *BMC genomics* 2010, 11: 379.
- [39] Cianciotto NP, White RC: Expanding Role of Type II Secretion in Bacterial Pathogenesis and Beyond. *Infection and immunity* 2017, 85 (5).
- [40] Liu H, Zhang S, Schell MA, Denny TP: Pyramiding unmarked deletions in *Ralstonia solanacearum* shows that secreted proteins in addition to plant cell-wall-degrading enzymes contribute to virulence. *Molecular plant-microbe interactions: MPMI* 2005, 18 (12): 1296-1305.
- [41] Genin S, Boucher C: Lessons learned from the genome analysis of *ralstonia solanacearum*. *Annual review of phytopathology* 2004, 42: 107-134.
- [42] Ghosh P: Process of protein transport by the type III secretion system. *Microbiology and molecular biology reviews: MMBR* 2004, 68 (4): 771-795.
- [43] Hueck CJ: Type III protein secretion systems in bacterial pathogens of animals and plants. *Microbiology and molecular biology reviews: MMBR* 1998, 62 (2): 379-433.
- [44] Hacker J, Carniel E: Ecological fitness, genomic islands and bacterial pathogenicity. A Darwinian view of the evolution of microbes. *EMBO reports* 2001, 2 (5): 376-381.
- [45] Silverman JM, Brunet YR, Cascales E, Mougous JD: Structure and regulation of the type VI secretion system. *Annual review of microbiology* 2012, 66: 453-472.
- [46] Zhang L, Xu J, Zhang H, He L, Feng J: TssB is essential for virulence and required for type VI secretion system in *Ralstonia solanacearum*. *Microbial pathogenesis* 2014, 74: 1-7.
- [47] Hikichi Y, Mori Y, Ishikawa S, Hayashi K, Ohnishi K, Kiba A, Kai K: Regulation Involved in Colonization of Intercellular Spaces of Host Plants in *Ralstonia solanacearum*. *Frontiers in plant science* 2017, 8: 967.